American Journal of Modern Physics
2023; 12(3): 30-46
http://www.sciencepublishinggroup.com/j/ajmp
doi: 10.11648/j.ajmp.20231203.11
ISSN: 2326-8867 (Print); ISSN: 2326-8891 (Online)

The Increasing of the Heat Transfer Coefficient of Short Linear Heat Pipes

Seryakov Arkady Vladimirovich

LLC 'Rudetransservice', Veliky Novgorod, Russia

Email address:
seryakovav@yandex.ru

To cite this article:
Seryakov Arkady Vladimirovich. The Increasing of the Heat Transfer Coefficient of Short Linear Heat Pipes. *American Journal of Modern Physics*. Vol. 12, No. 3, 2023, pp. 30-46. doi: 10.11648/j.ajmp.20231203.11

Received: October 3, 2023; **Accepted**: October 24, 2023; **Published**: November 17, 2023

Abstract: The results of the experimental studies of heat transfer coefficients K_{HP} of short linear heat pipes (HP's) with a Laval nozzle-liked vapour channel, and with a partially swirled vapour flow inside the channel are presented. A partial azimuthal swirling of the jet vapour stream is created using inclined injection channels 1 mm in diameter in a flat multilayer mech evaporator, with an inclination angle φ relative to the longitudinal axis in the azimuthal direction, in the range of $0° < φ < 60°$. The heat transfer coefficients K_{HP} of a set of the identical HP's with a different inclination angles φ of the injection channels in the evaporators, with the same working fluid mass filling ($δm/m \leq 0.1$ %), at the same evaporator temperature heat load $δT = T_{ev} - T_B = (20 \pm 0.03)$ K, represent an extreme convex function, depending on the inclination angle φ magnitude of the injection channels, with a maximum at the swirled angle of the vapour flow $φ = 26° \pm 2°$. The magnitude of the excess of the K_{HP} with a swirling vapour flow over the identical HP's with a direct vapour flow reaches 10%. An analysis of the recommended vapour channel shape, carried out by the estimating of the Richardson number Ri of the vapour flow jets above the evaporator, allowed us to estimate the value of the dimensionless longitudinal radius of curvature $δ/R_{conf}$ of the confuser part of the vapour channel, which is determined from the condition of minimal friction losses during the flow of moist vapour in the boundary layer δ along the concave wall of the confuser part of the vapour channel with a longitudinal radius of curvature R_{conf}. The concave diffuser part shape of the vapour channel is determined by the condition that the moving vapour jets velocity vectors must be parallel to the longitudinal axis of the diffuser part of the HP's vapour channel. The results of the numerical simulation of the hydraulic resistance coefficients $ξ_{vp}$ of the HP's vapour channel, closed with flat covers, with partially swirling jet vapour flow, obtained by using the ANSYS FLUENT program, show a decrease in $ξ_{vp}$ coefficients at high values of the evaporator temperature load, in the range of vapour flow velocities 1 m/s $< u_z \leq$ 100 m /s, and in the range of swirling angles $0°<φ<30°$. With the increasing the swirling angles $φ>30°$, a sharp increase in the hydraulic resistance coefficient $ξ_{vp}$ begins.

Keywords: Short Linear HP's, Azimuthal Swirling of the Vapour Jets, Hydraulic Resistance Coefficient

1. Introduction

The increasing of the HP's heat transfer coefficient is a complex scientific and technological problem, several solutions for which were proposed and considered in detail by many authors earlier [1-8].

Short line HP's are important and widely used heat transfer devices, primarily for space cooling applications. In the Russian Federation, Roscosmos and Rosatom have developed spacecraft and satellites with a nuclear power propulsion systems (NPPS) as a part of the Transport and Energy Module (TEM) program. To cool heat-stressed structures of nuclear power plants, linear heat transfer systems, based on a short HP's, with a Laval nozzle-liked vapour channel, with flat covers and phase transitions, localized on them, with strict take-off mass regulation, and with excess heat radiation into the surrounding space, are also in demand. To further increase the heat transfer coefficients K_{HP} of such HP's, intensify the internal condensation and evaporation processes, the various methods are used to increase the efficiency [1-5], and heat transfer of the HP's [6-8]. One of the proposed methods is a method, based on swirling the vapour flow over a flat evaporator in the vapour channel of short HP's.

The control of heat and mass transfer processes due to the organization of the flows aerodynamics in the vapour channel, in particular, by swirling the flow of moist vapour over the evaporator of short HP's, is an extremely promising way to intensify the heat transfer K_{HP} of short HP's with a Laval nozzle-liked vapour channel.

Swirling flows of liquid and vapour media are widely represented in various power and thermal machines and devices [9-14], including in cooling devices. The use of the swirling motion of vapour to intensify the processes of condensation, evaporation and overheating of moist vapour above the HP's evaporator, and the transfer of heat and mass in the vapour channel and boundary layer leads to the appearance of new interesting effects.

The use of such short HP's with a swirling vapour flow is justified in the case of structural impossibility of placing loop HP's, as well as to increase the long-term stability and reliability of cooling systems for space objects subjected to intense meteorite impact with nuclear power plants, in which there are no externally distributed inlet and outlet lines of loop HP's.

Partial swirling of vapour jets above the evaporator in the vapour channel of short HP's, 100 mm long and 20 mm in diameter, made in the Laval nozzle – liked form, at high temperature loads on the evaporator, and accounting of all three components of the vapour flow velocity u according to the formula (1):

$$u = \sqrt{u_z^2 + u_r^2 + u_\varphi^2} \qquad (1)$$

leads to a decrease in the hydraulic resistance coefficient ξ_{vp}, when moist vapour moves in the vapour channel in a certain range of swirling angles $\Delta\varphi$.

In addition, a partial swirling of the vapour flow in the Laval nozzle-liked vapour channel of short HP's at a high temperature evaporator loads, leads to additional azimuthal rotation of the formed toroidal vortex of the condensing vapour, intensification of vapour condensation on the flat surface of the HP's top cover, and an increase in the heat transfer coefficient K_{HP} of our HP's.

2. Method and Materials

Short HP's with a Laval nozzle –liked vapour channel were previously presented in detail when publishing the results of various studies [4, 5, 6, 16, 17], and is well-known.

Therefore, we will not repeat the descriptions of the HP's design with all the details in the measuring sensors and their calibrations, but will focus on a detailed analysis and consideration of the required shape of the HP's vapour channel.

A schematic diagram of the experimental test setup is shown in Figure 1. In the upper cover capacitive sensors are installed to measure the working fluid condensate film thickness and temperature [16, 17].

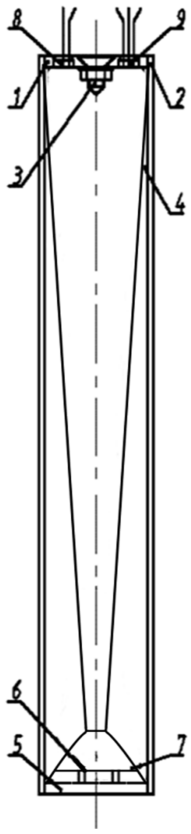

Figure 1. *HP's diagram. 1 – top cover; 2 – cylinder body of the HP's; 3 – locking element; 4 – multilayer mesh capillary-porous insert with uniform dense radial cross-linking; 5 – bottom cover; 6 – capillary injector channels with a diameter of 1 mm; 7– bottom flat multilayer mesh evaporator. There are capacitance sensors 8, 9, 10 installed inside the top cover [4-6], two of which are intended for a condensate film thickness measurement, while the third with a welded on its electrodes microthermistor CT3-19 to measure the film temperature.*

2.1. HP's Evaporator Operations

The determining the shape of a concave vapour channel of short HP's with a Laval nozzle –liked form and intended for use at high temperature evaporator loads, when working in spacecraft and satellites with nuclear power plants, is an important practical task. The swirling flow intensifies the transfer processes in the boundary layer in the channel, due to an increase in velocity gradients and an increase in turbulent transfer in the mass forces field.

Swirling (twirled) currents, including partially swirling moist vapour currents, belong to the class of spatial boundary layers [7-12]. When analyzing the swirling flow, we use the method of straightening current lines and its analogues, developed and presented in detail in [9-13]. In these works, it is shown that heat and mass transfer and hydraulic resistance during the longitudinal and swirling turbulent flows in the HP's vapour channel initial section can be described by the same functional dependencies, using the so-called effective Reynolds number Re_{eff}, determined by the formula:

$$Re_{eff} = Re\sqrt{(1 + tg^2\varphi)};\ Re = \frac{u\rho_{vp}^{mix}D}{\mu_{vp}^{mix}} \qquad (2)$$

where φ is the swirling twist angle of the vapour flow, determined by the ratio of the azimuthal and longitudinal velocity components, and set by the inclination angle of the injection channels 1 mm in diameter, in a multilayer mesh evaporator with a 3.5 mm total thickness, to the longitudinal axis of the HP.

The velocity components above the evaporator are defined as the velocity values near the outlet openings of the injection channels in the following form - $u_z \sim u_\varphi \cdot \mathrm{Cos}\varphi$ – the longitudinal component of the vapour velocity above the HP's evaporator, m/s; $u_r \sim u_\varphi \cdot \mathrm{Sin}\varphi$ –the radial component of the vapour velocity above the HP's evaporator, m/s; u_φ – the azimuthal component of the vapour velocity above evaporator at the mouth of the injection channels, m/s.

The standard Navier-Stokes equations of motion and energy for the boundary layer of an incompressible flow of moist vapour above the evaporator at the HP's initial section, in a cylindrical coordinate system are written in the following form [14, 15]:

$$\rho_{vp}^{mix}\left(u_r\frac{\partial ru_\varphi}{\partial r}+u_z\frac{\partial ru_\varphi}{\partial z}+\frac{u_\varphi}{r}\frac{\partial ru_\varphi}{\partial \varphi}\right)=-\frac{\partial p}{\partial \varphi}-\frac{1}{r}\frac{\partial\left(\rho r^2\overline{u'_\varphi u'_r}\right)}{\partial r}+\frac{1}{r}\frac{\partial[\mu r^3\,\partial(u_\varphi/r)/\partial r]}{\partial r}. \quad (3)$$

$$\rho_{vp}^{mix}\left(u_r\frac{\partial u_z}{\partial r}+u_z\frac{\partial u_z}{\partial z}+\frac{u_\varphi}{r}\frac{\partial u_z}{\partial \varphi}\right)=-\frac{\partial p}{\partial z}-\frac{1}{r}\frac{\partial\left(\rho_{vp}^{mix}r^2\overline{u'_r u'_z}\right)}{\partial r}+\frac{1}{r}\frac{\partial[\mu r\,\partial u_z/\partial r]}{\partial r}. \quad (4)$$

$$\frac{\partial\rho_{vp}^{mix}ru_r}{\partial r}+\frac{\partial\rho_{vp}^{mix}ru_z}{\partial z}+\frac{1}{r}\frac{\partial\rho_{vp}^{mix}ru_\varphi}{\partial \varphi}=0. \quad (5)$$

$$\rho_{vp}^{mix}C_p^{mix}\left(u_r\frac{\partial T}{\partial r}+u_z\frac{\partial T}{\partial z}+\frac{u_\varphi}{r}\frac{\partial T}{\partial \varphi}\right)=-\frac{1}{r}\frac{\partial\left(\rho_{vp}^{mix}C_p^{mix}r^2\overline{u'_r T'}\right)}{\partial r}+\frac{1}{r}\frac{\partial}{\partial r}\left(\lambda_{vp}^{mix}r\frac{\partial T}{\partial r}\right). \quad (6)$$

The components of the tangential stresses and heat flow in the vapour channel can be written as follows:

$$\tau_{r\varphi}=-\rho_{vp}^{mix}\overline{u'_\varphi u'_r}+\mu_{vp}^{mix}r\frac{\partial(u_\varphi/r)}{\partial r} \quad (7)$$

$$\tau_{rz}=-\rho_{vp}^{mix}\overline{u'_r u'_z}+\mu_{vp}^{mix}\frac{\partial u_z}{\partial r} \quad (8)$$

$$q_r=-\rho_{vp}^{mix}C_p^{mix}\overline{u'_r T'}+\lambda\frac{\partial T}{\partial r} \quad (9)$$

The equation for determining the longitudinal component of the heat flow inside the vapour channel near the HP's condensation surface, can be written as follows:

$$q_z=-\rho_{vp}^{mix}C_p^{mix}\overline{u'_z T'}+\lambda_l\frac{\partial T}{\partial z}. \quad (10)$$

The above boundary layer equations (3) – (6), presented here in a cylindrical coordinate system, can be written in the coordinates of the swirling current lines on the surface of the HP's vapour channel. These coordinates associated with the current line along the surface of the Laval nozzle–liked vapour channel, are written in the following form:

$$u_\ell=\frac{u_z}{\cos\varphi};\ \tau_{y\ell}=-\frac{\tau_{rz}}{\cos\varphi};\ d\ell=\frac{dz}{\cos\varphi};\ \varphi=\mathrm{arctg}\frac{u_\varphi}{u_z}. \quad (11)$$

where φ is the swirling angle between the current line of the vapour jet, and the longitudinal z axis.

Using these coordinates of the swirling lines (11), for a thin boundary layer $\delta/R << 1$, the equations of the boundary layer energy and motion [14, 15] are written as follows:

$$\rho_{vp}^{mix}u_y\frac{\partial u_\ell}{\partial y}+u_\ell\frac{\partial u_\ell}{\partial \ell}=-\frac{\partial p}{\partial \ell}+\frac{\partial\tau_{y\ell}}{\partial y} \quad (12)$$

$$\frac{\partial\rho_{vp}^{mix}u_y}{\partial y}+\frac{\partial\rho_{vp}^{mix}u_\ell}{\partial \ell}=0. \quad (13)$$

$$\rho_{vp}^{mix}C_p^{mix}\left(u_y\frac{\partial T}{\partial y}+u_\ell\frac{\partial T}{\partial \ell}\right)=\frac{\partial q_y}{\partial y}. \quad (14)$$

Thus, the defining equations of the swirling moist vapour flow motion and energy on the boundary layer, written in coordinates, associated with the current line of the swirling jets, completely coincide with the boundary layer equations for the standard uncoiled flow over the HP's evaporator of radius R_{ev}, with the longitudinal coordinate ℓ and the velocity of the undisturbed flow u_ℓ. The maximum value of the total evaporation rate of a moist vapour over a capillary-porous evaporator (CPE) is determined by a standard method [16, 17]:

$$\dot{M}=G_{mix}=G_{vp}+G_{dr}=\dot{n}_{vp}m_{vp}=F_{ev}(z)\rho_{vp}^{mix}(T_{ev})u=\frac{Q_{ev}}{r(T_B)}=4.4\cdot10^{-4}\ \mathrm{kg/s}. \quad (15)$$

All details of the HP's CPE operation with the injection channels are given in [16, 17]. The boundary conditions for solving the Navier-Stokes equations, energy and mass, and motion of the boundary layer (4) – (15) in the HP's vapour channel, are given in [5, 6]. For two-phase moist vapour flow with a density of ρ_{vp}^{mix} over the completely filled with diethyl ether evaporator outer surface, at the beginning of the evaporation, the vapour flow rate and flow velocity are equal to:

$$z=L_{ev}:\ \lambda_{ev}\frac{\partial T_{ev}}{\partial n}\Big|_{\Omega_{ev-}}-\lambda_{ev}\frac{\partial T_{ev}}{\partial n}\Big|_{\Omega_{ev+}}=G_{mix};\ u_z=\frac{u_{vp}}{u_{ev}};\ u_r=\frac{v_{vp}}{v_{ev}};\ u_\varphi=\frac{w_{vp}}{w_{ev}},\rho=\rho_{vp}^{mix}. \quad (16)$$

at the interface of the pairs – the inner surface of the insert $\Omega(\bar{z})$ (adhesion condition):

$$x=y=\Omega(\bar{z}),\bar{z}=\frac{z}{R^*}:\ u_z=0,\ u_r=0,\ u_\varphi=0;\ \frac{\partial\rho_{vp}^{mix}}{\partial y}=\frac{\partial\rho_{vp}^{mix}}{\partial x}=0;\gamma_{dr}=0.2 \quad (17)$$

on the axis of the nozzle symmetry (symmetry condition):

$$x=0,\ y=0:\ \frac{\partial u}{\partial y}=\frac{\partial u}{\partial x}=0;\ \frac{\partial\rho_{vp}^{mix}}{\partial y}=\frac{\partial\rho_{vp}^{mix}}{\partial x}=0 \quad (18)$$

on the condensation surface (inner surface of the flat top cover):

$$z=L_{HP}-\delta_{film}:\ \frac{\partial u}{\partial z}=0,\frac{\partial v}{\partial z}=0,\frac{\partial w}{\partial z}=0,\frac{\partial\rho_{vp}^{mix}}{\partial z}=0. \quad (19)$$

Integral relations for the boundary layer of a curved coordinate system can be obtained by integrating equations (12) – (14) over the thickness of the boundary layer δ, using standard transformations [18-21].

With a gradient-free flow around the wall surface of the vapour channel by a swirling vapour flow, the so-called integral relations can be represented in the usual way in the form of the friction coefficient $C_{f\ell}$ and the Stanton number St_ℓ in the following form:

$$\frac{d\delta_\ell^{**}}{d\ell} = \frac{1}{2}C_{f\ell} \ . \quad (20)$$

$$\frac{d\delta_{t\ell}^{**}\rho_{vp}^{mix}C_p^{mix}u_\ell\Delta T}{\rho_{vp}^{mix}C_p^{mix}u_\ell\Delta T d\ell} = St_\ell \ . \quad (21)$$

The integral parameters for equations (12) – (14) for the moist vapour flow are written as the thickness δ_ℓ^{**} of the momentum loss and the thickness $\delta_{t\ell}^{**}$ of the energy loss of the longitudinal swirling flow along the current lines as follows:

$$\delta_\ell^{**} = \int_0^\delta \frac{\rho_{vp}^{mix}u_\ell}{\rho_{vp0}^{mix}u_{\ell 0}}\left(1 - \frac{u_\ell}{u_{\ell 0}}\right)dy. \quad (22)$$

$$\delta_{t\ell}^{**} = \int_0^\delta \frac{\rho_{vp}^{mix}u_\ell}{\rho_{vp0}^{mix}u_{\ell 0}}\left(1 - \frac{T-T_{wall}}{T_0-T_{wall}}\right)dy. \quad (23)$$

In this case, the friction and heat exchange coefficients along the current lines are determined in the usual way:

$$\frac{1}{2}C_{f\ell} = \frac{\tau_{y\ell}}{\rho_0 u_{\ell 0}^2}; \ St_\ell = \frac{q_{wall}}{\rho_{vp}^{mix}C_p^{mix}u_{\ell 0}(T_0 - T_{wall})} \ . \quad (24)$$

As a determining parameters, the coefficients of friction and heat and mass transfer of the swirling flow of the HP's moist vapour, include the full velocity $u_{\ell 0}$ at the boundary of the boundary layer. The integral relations (20) and (21), which determine the coefficients of friction and heat and mass transfer of the swirling vapour flow inside the HP's channel, are completely isostructured to the corresponding equations for the case of a flow without swirling [21-23]. Therefore, the solutions of equations (20) and (21) will also be similar if the moist vapour flow criteria included in them are calculated using the full velocity $u_{\ell 0}$ and the current line length ℓ.

Special Reynolds numbers are introduced, the first based on the thickness of the pulse loss along the current line Re_ℓ^{**} and the second Reynolds number based on the thickness of the energy loss along the current line $Re_{t\ell}^{**}$:

$$\frac{1}{2}C_{f\ell} = \frac{B}{2}(Re_\ell^{**})^{-0.25}\Psi_t\Psi_k; Re_\ell^{**} = \rho_{vp}^{mix}u_{\ell 0}\delta^{**}/\mu_{vp0}^{mix}. \quad (25)$$

$$St_\ell = \frac{B}{2}(Re_{t\ell}^{**})^{-0.25}Pr^{-0.75}\Psi_t\Psi_{kt}; Re_{t\ell}^{**} = \rho_{vp}^{mix}u_{\ell 0}\delta_t^{**}/\mu_{vp0}^{mix}. \quad (26)$$

The parameters distribution of the boundary layer of the swirling vapour flow at constant values of friction and heat and mass transfer along the length of the HP's vapour channel in the first approximation can be determined as follows:

$$\delta_\ell^{**} = \left(\frac{B(1+m)}{2}\Psi_t\Psi_k\right)^{0.8}\ell\, Re_\ell^{-0.2}; Re_\ell = \rho_{vp}^{mix}u_\ell\ell/\mu_{vp}^{mix}. \quad (27)$$

$$\frac{C_{f\ell}}{2} = \frac{\delta_\ell^{**}}{\ell(1+m)}; \ m = 0.25 \quad (28)$$

For a thermal boundary layer with a constant value of the heat flux q_{wall} = const, similar functional dependences of the boundary layer parameters can be written as:

$$\delta_{t\ell}^{**} = \left(\frac{B}{2}\Psi_t\Psi_{kt}\right)^{0.8}Pr^{-0.6}\ell\, Re_\ell^{-0.2}; Re_\ell = \rho_{vp}^{mix}u_\ell\ell/\mu_{vp}^{mix} \quad (29)$$

$$St_\ell = \frac{\delta_{t\ell}^{**}}{\ell} \quad (30)$$

To analyze the obtained equations (25)–.(30), which determine the main parameters of the boundary layer – its thickness, friction and heat and mass transfer coefficients of the swirling vapour flow in the layer, they are expressed in terms of the defining parameters of the uncoiled vapour flow. We use the axial component of the moist vapour flow velocity at the outer boundary of the boundary layer u_{z0} and the longitudinal z coordinate of the axisymmetric vapour channel. Taking into account equations (24), we obtain the following expressions for the boundary layer thickness and the friction coefficient:

$$\delta_\ell^{**} = \delta^{**} = \left(\frac{B(1+m)}{2}\Psi_t\Psi_k\right)^{0.8}Re_z^{-0.2}z\cos\varphi^{-0.6} \quad (31)$$

$$\frac{1}{2}C_{fz} = \frac{C_{f\ell}}{2}\frac{1}{\cos\varphi} = \frac{1}{(1+m)^{0.2}}\left(\frac{B}{2}\Psi_t\Psi_k\right)^{0.8}Re_z^{-0.2}\cos\varphi^{-0.6} \quad (32)$$

In equations (31) – (32), the Reynolds number and the friction coefficient are determined as follows:

$$Re_z = \rho_{vp}^{mix}u_{z0}z/\mu_{vp}^{mix}; \ \frac{1}{2}C_{fz} = (\tau_{yz})_{wall}/\rho_{vp}^{mix}u_{z0}^2 \quad (33)$$

To evaluate the heat transfer on the vapour channel surface, we write out the equations for the thickness of the energy loss with an uncoiled flow in the same way:

$$\delta_t^{**} = \left(\frac{B}{2}\Psi_t\Psi_{kt}\right)^{0.8}Pr^{-0.6}Re_z^{-0.2}z\cos\varphi^{-0.6} \quad (34)$$

$$St = \frac{q_{wall}}{\rho_{vp}^{mix}C_p^{mix}u_z\Delta T} = \left(\frac{B}{2}\Psi_t\Psi_{kt}\right)^{0.8}Pr^{-0.6}Re_z^{-0.2}\cos\varphi^{-0.6} \quad (35)$$

Thus, the coefficient of heat and mass transfer on the wall during the flow of a partially swirled stream of moist vapour in the HP's vapour channel, and the friction stress in the axial direction of the also partially swirled stream is greater, than in the not swirling flow by $\cos\varphi^{-0.6}$ times at the same distance from the evaporator surface, and the same longitudinal velocity component at the boundary of the boundary layer. At the same time, in the first approximation, we do not take into account the additional impact of mass forces due to the vapour flow swirled on the turbulent transfer, we consider the relative friction coefficients to be constant:

$$\Psi_t = \Psi_{kt} = 1 \quad (36)$$

The analysis of the boundary layer equations using the

well-known principle of straightening the current lines [20-23] shows that the processes of heat and mass transfer and friction in a swirling vapour flow are similar, and the amount of friction of the moist vapour flow in the axial direction increases like the amount of heat transfer, according to (29) and (30).

However, the results of experimental studies [22, 23] show a significantly greater increase in hydraulic resistance in a swirling flow, compared with an increase in heat transfer. This is due to the fact, that the value of ξ_{vp} in these studies was determined by the loss of total pressure during flow in the channel, which consists of friction losses during flow in the longitudinal and azimuthal directions.

We compare the thickness of the boundary layers of the flow with a swirled and without a swirled at the same Reynolds numbers, determined by the magnitude of the total velocity and by the momentum loss thickness along the current line:

$$\mathrm{Re}_{\ell}^{**} = \rho_{vp}^{mix}\frac{u_{\ell 0}\delta^{**}}{\mu_{vp}^{mix}} \equiv \mathrm{Re}_{\ell}^{**} = \frac{\delta^{**}\rho_{vp}^{mix}u_{zo}}{\mu_{vp0}^{mix}}; \delta_t^{**} = \delta^{**} \qquad (37)$$

Then the relative coefficients of heat and mass transfer and friction for a swirling vapour flow can be expressed as follows:

$$\Psi = \left(\frac{C_{fz}}{C_{f0}}\right)_{Re_{\ell}^{**}} = \left(\frac{St}{St_0}\right)_{Re_{t\ell}^{**}} = \frac{1}{\cos\varphi} \qquad (38)$$

Thus, it can be considered established that the laws of heat and mass transfer and friction in a swirling stream of moist vapour inside the HP's, obtained by applying the principle of straightening current lines [20-23], coincide with the same dependencies, obtained using the Prandtl hypothesis [22, 23] for the spatial boundary layer, and they allow us to apply a partially swirled flow in the vapour channel to increase the HP's heat transfer coefficients K_{HP}.

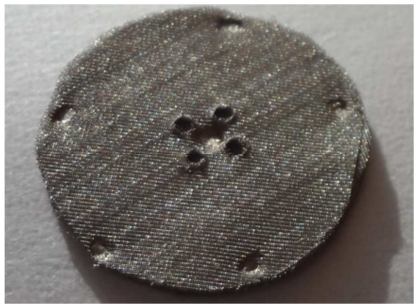

Figure 2. *Image of one of the billets of a multilayer capillary-porous HP's evaporator with a cell size of 0.04 mm. Four injection channels with a diameter of 1 mm are clearly visible for the exit and formation of vapour jets, penetrating through round work pieces with 10 layers of mesh in each.*

Multilayer mesh capillary-porous evaporator (CPE) is a set of blank blocks, welded by contact spot welding to the HP's bottom cover, with a total thickness of 3.5 mm. Each of the blocks is made of 10 layers of metal mesh 0.07 mm thick, with a cell size of 0.04 mm. Figure 2 shows one of these blocks with injection channels. The final evaporator with a thickness of 3.5 mm allows you to reliably form the azimuthal angle of inclination of the injection channels in the range of $\varphi = 0° - 60°$.

For partial twirled and overheating of the swirling vapour flow, four inclined injection channels with 1 mm diameter are used in a flat evaporator, the outlet holes of which are located at a diameter of $2r_4$, inside the nozzle diameter of critical section d_{cr}, $2r_4 \le d_{cr}$.

The value of the swirling integral parameter $S = {M_{z\varphi}}/{M_z \cdot r_4}$ achievable in this evaporator, is considered in the 3[d] paragraph.

A slight attenuation of the tangential swirling of the jet vapour flow due to friction, increases the static pressure in the axial part, and decreases in the peripheral part of the vapour flow in the Laval nozzle-liked vapour channel, which increases the stability and turbulence degree of the condensed vapour flow, and increases the heat transfer coefficient K_{HP} of our HP's.

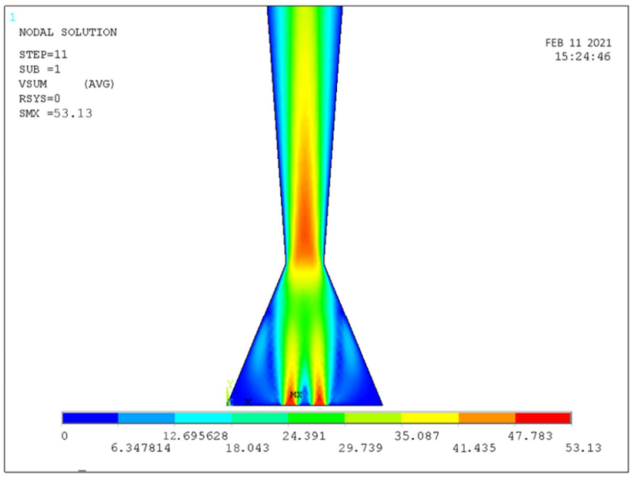

Figure 3. *The forward direction of the injection vapour channels, the angle of inclination to the longitudinal axis φ = 0 °. The evaporator overheating relative to the boiling point of diethyl ether is set to $\delta T = T_{ev} - T_B = 15K$, vapour velocity in m/s.*

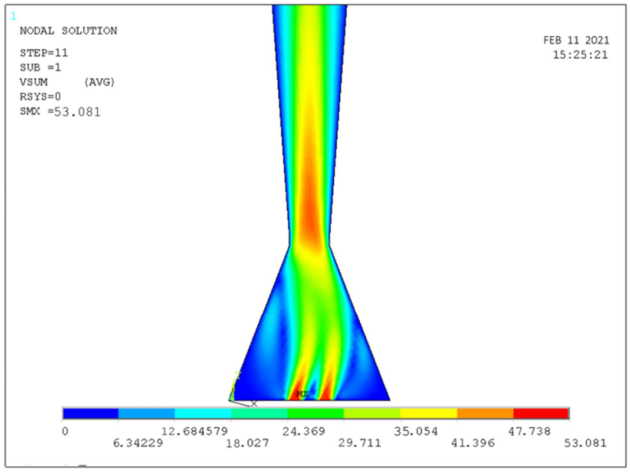

Figure 4. *Moist vapour flow mode. The angle of the injection vapour channels inclination to the longitudinal axis in the azimuthal direction is φ = 15°. The evaporator overheating relative to the boiling point of diethyl ether is set to $\delta T = T_{ev} - T_B = 15K$, vapour velocity in m/s.*

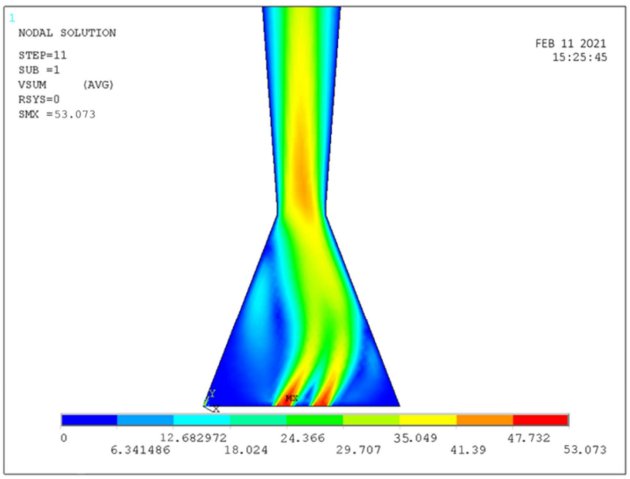

Figure 5. *Moist vapour flow mode. The angle of the injection vapour channels inclination to the longitudinal axis in the azimuthal direction is φ = 30°. The evaporator overheating relative to the boiling point of diethyl ether is set to δT = T_{ev} –T_B = 15K, vapour velocity in m/s.*

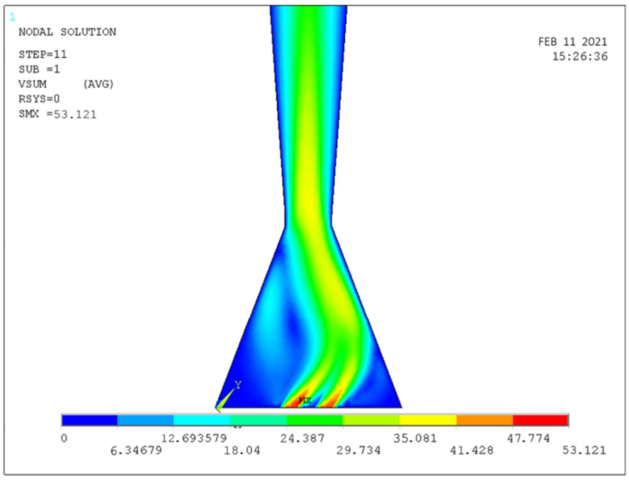

Figure 6. *Moist vapour flow mode. The angle of the injection vapour channels inclination to the longitudinal axis in the azimuthal direction is φ = 45°. The evaporator overheating relative to the boiling point of diethyl ether is set to δT = T_{ev} –T_B = 15K, vapour velocity in m/s.*

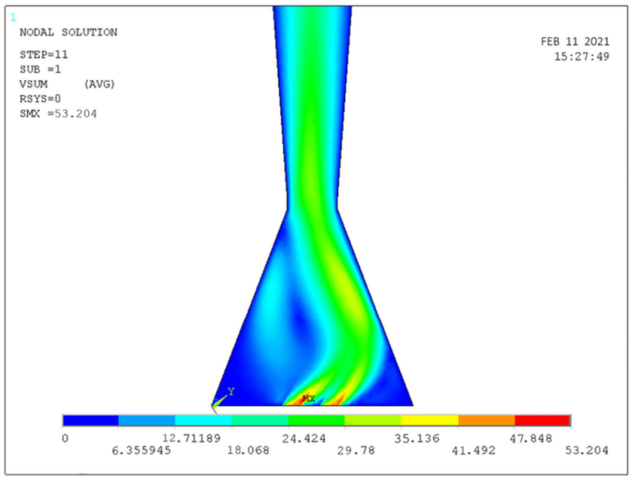

Figure 7. *Moist vapour flow mode. The angle of the injection vapour channels inclination to the longitudinal axis in the azimuthal direction is φ = 55°. The evaporator overheating relative to the boiling point of diethyl ether is set to δT = T_{ev} –T_B = 15K, vapour velocity in m/s.*

Figures (3–7) show the moist vapour flow mode with a humidity coefficient y_{dr} = 0.2, from a capillary-porous evaporator with through injection channels with 1 mm diameter, in the entire range of inclination angles φ = 0 ° – 60°, designed for the output and formation of vapour jets above the flat evaporator surface at high thermal loads.

Capillary-Porous Evaporator (CPE) and Capillary-Porous Insert (CPI) are connected by contact welding and form a single hydraulic system for the delivery of diethyl ether from CPI to CPE. Inclined injection channels allow you to create a partially swirled vapour flow over a HP's flat evaporator.

Large values of the superheated vapour velocity above the injection channels, are accompanied by large values of the dynamic pressure P_{dyn} in them, and lead to a decrease the static pressure P_{stat} in the channels, and the horizontal flow of diethyl ether in the gaps along the layers of the metal mesh of the CPE, into these injection channels from the CPI, surrounding the CPE.

The heat transfer α_{ev} during diethyl ether boiling in a multilayer CPE [16, 17, 24] is estimated by the formula:

$$\propto_{ev} \sim Aq_{ev}^{2/3} \qquad (39)$$

The conducted studies on our HP's give the following values: A ~ 1; $a_{ev} = 2.3 \cdot 10^4$ W/Km^2 at a heat load of $\delta T = T_{ev} - T_B = 20K$.

The expression for the thermal energy released in the HP's evaporator, is written using the heat balance equation:

$$q_{ev} - G_{vp}\, r(T_B)\frac{dx_{ev}}{dz}L_{ev} - G_{vp}\,(1 - x_{ev})C_p^{mix}\frac{dT_{fev}}{dz}L_{ev} - \lambda_{sc}(1 - \Pi)\frac{d^2T_{sc}}{dz^2}F_{ev}(z)L_{ev} = 0. \qquad (40)$$

The vapour flow can be estimated according to the interphase mass transfer, gives in case of small departures from equilibrium by the Hertz - Knudsen equation [16, 17]:

$$G_{vp} = \frac{2\zeta}{2-\zeta}\left(\frac{M}{2\pi R}\right)^{1/2}\left(\frac{P_{ev}}{\sqrt{\overline{T}_{fev}}} - \frac{P_{fcond}}{\sqrt{\overline{T}_{fcond}}}\right);\ \zeta \le 1. \qquad (41)$$

The enthalpy equation of a working evaporator in a stationary state looks like this:

$$H_{ev} = G_{vp}r(T_B) + G_{vp}C_{vp}(T_{ev} - T_{sc}) + G_lC_{pl}(T_{ev} - \overline{T}_{fev}) \qquad (42)$$

The measurements carried out at maximum heating and the average temperature $\overline{T}_{TT}$ = 320.45 K (47.3 °C) of the HP's outer surface, electrical power and temperature of the resistive heater T_H = 353.15 K (80 °C), the contribution values are as follows: $G_{vp} = 4.4 \cdot 10^{-4}$ kg/s; heating of liquid diethyl ether $C_l(T_{ev} - \overline{T}_{fev})$ ~ 12.6 W (or 10%), vapour overheating $C_{pv}(T_{ev} - T_{sc})$ ~ 2.5W (or 2%) of the incoming thermal power Q_{ev}, W. All the details of the evaporator operation analysis and the evaluation of the terms of equations (40), (41) of short HP's with injection channels are given in [16, 17, 24].

2.2. The Shape of the Vapour Channel

The shape of the HP's vapour channel is chosen as a closed nozzle, close to the Laval nozzle, with flat upper and lower covers. The confuser part of the closed nozzle, operating in the acceleration mode of the moist vapour flow of short low-temperature HP's evaporating over a flat multilayer mesh evaporator, with an injection capillary channels, is limited by the region of subsonic moist vapour flow velocities, and small values of the Richardson number Ri.

The shape of the HP's vapour channel should be determined based on the condition of minimal friction energy losses during subsonic flow of moist vapour over the evaporator, primarily along the concave walls inside the boundary layer both in the confuser and diffusor parts of the vapour channel. It is necessary to specify the shape of the channel and the radii of longitudinal curvature in the confuser R_{conf} and in the diffusor R_{diff} parts of the nozzle with subsonic moist vapour flow, taking into account the three-dimensional flow structure and emerging secondary currents.

2.3. The Confuser Part of the Vapour Channel

To consider our problem of estimating the surface shape of a concave section of the confuser, made in the form of a fragment of a closed nozzle close to the Laval nozzle with flat covers, forming a vapour channel of a short linear HP's, and analyzing complex flows in this fragment of the HP's vapour channel, we will apply the Richardson number Ri [18-20]:

$$\mathrm{Ri} = 2\mathrm{u}/\frac{\partial(\mathrm{ur})}{\partial \mathrm{r}} \tag{43}$$

Many authors have modernized and improved this parameter, for example, which is the ratio of the buoyancy force in the gravity field g of the Earth to the inertia of the motion of a dense medium; the ratio of the stratification of a dense medium, for example, moist vapour also in the gravity field g in a vertically oriented HP's vapour channel to the influence of the radial gradient of flow velocity; the turbulent Richardson number was also proposed, taking into account the turbulence kinetic energy k and the dissipation rate ε in the following form:

$$\mathrm{Ri} = -\frac{g}{\rho_{vp}^{mix}}\frac{\partial \rho_{vp}^{mix}}{\partial r}\Big/\left(\frac{\partial \mathrm{u}}{\partial r}\right)^2;\ \mathrm{Ri} = \frac{k^2}{\varepsilon^2}\frac{\mathrm{u}}{r^2}\frac{\partial(\mathrm{ur})}{\partial \mathrm{r}} \tag{44}$$

This parameter, the turbulent Richardson number, which determines the ratio of the turbulent energy production by mass forces to the production of turbulent energy by tangential stresses during the moist vapour flow over the evaporator inside the confuser part of the closed nozzle, will allow us to estimate the surface shape of the HP's confuser part of the vapour channel.

In this case, mass forces can be caused not only by the vapour flow circulation gradient, but also by the density gradient of this flow in the boundary layer on the inner surface of the confuser part of the closed HP's vapour channel, and the Richardson number is recorded and calculated using a more general formula:

$$\mathrm{Ri} = \left[2\frac{\mathrm{u}}{\mathrm{r}^2}\frac{\partial(\mathrm{ur})}{\partial \mathrm{r}} + \frac{1}{\rho}\frac{\partial \rho}{\partial \mathrm{r}}\frac{\mathrm{u}^2}{\mathrm{r}}\right]\Big/\left[\frac{1}{\mathrm{r}}\frac{\partial(\mathrm{ur})}{\partial \mathrm{r}}\right]^2 \tag{45}$$

The Richardson number is a local characteristic of the vapour flow along a curved confuser surface, and its value varies along the thickness of the boundary layer from zero on the wall surface, to the highest value on the outer boundary of the layer. For a flow in a boundary layer on a curved surface with a constant moist vapour density $\rho_{vp}^{mix} = \mathrm{const}$, the expression (45) is significantly simplified and coincides with the standard form of the Richardson number (43) [19, 20].

The profile of the confuser part of the nozzle (profiling) should be constructed taking into account the requirement of minimal energy losses of the moist vapour, when moving inside the concave surface of the confuser part of the closed HP's vapour channel, and an attempt to briefly estimate its radius will be given below.

Heat losses into the nozzle wall weaken the influence of the longitudinal radius of curvature of the channel R_{ch} on the convergence process (concentration) of the turbulent vapour flow, and its absolute value $G_{vp} = \rho_{vp}^{mix}\, u$, and near the surface of the concave confuser channel, the loss value is recorded as follows:

$$q_{wall} = C_p^{mix}\rho_{vp}^{mix}\,\overline{T'u_r'} = C_p^{mix}\,\rho_{vp}^{mix}\,\ell_0^2\,\frac{\partial T}{\partial r}\left[\frac{1}{r}\frac{\partial(ur)}{\partial r}\right]\Big/\sqrt{1-\left(\frac{y}{\ell_0}\right)^2\mathrm{Ri}}\,. \tag{46}$$

The heat flow on the concave surface is closely related to the distribution of turbulent tangential stresses, and the magnitude of this stress τ_{zx} over the thickness of the curved boundary layer on the confuser concave surface is as follows:

$$\tau_{zx} = \rho_{vp}^{mix}\,\overline{u'u'_{r0}}\sqrt{1-\left(\frac{y}{\ell_0}\right)^2\mathrm{Ri}} = \rho_{vp}^{mix}\,\ell_0^2\left[\frac{1}{r}\frac{\partial(ur)}{\partial r}\right]^2\sqrt{1-\left(\frac{y}{\ell_0}\right)^2\mathrm{Ri}}\,. \tag{47}$$

Thus, by applying the relations (45), (46), and (47), it is possible to take into account the effect of curvature on heat and mass transfer and friction during turbulent flow around concave and convex surfaces. Prandtl [19] was one of the first to propose a formula for estimating turbulent friction based on the Richardson number [19-23], using the theory of the mixing path length, as a result, the amount of friction is estimated as follows:

$$\frac{\tau}{\tau_0} = \sqrt{(1-0.5\mathrm{Ri})};\ \mathrm{Ri} = \frac{2u}{(\partial ur/\partial r)} \tag{48}$$

To estimate the magnitude of the effects caused by the curvature of the vapour flow lines, the dynamic viscosity coefficient of moist vapour is multiplied by the damping function, associated with the Richardson number of the flow [21-23] as follows:

$$\mu = \mu_{vp} f(Ri);\ f(Ri) = \sqrt{(1 - \xi\, Ri)};\ \xi \sim 0.1;\ \mu = 0.93\mu_{vp} = 7.5 \cdot 10^{-6}\ Pa \cdot s \quad (49)$$

The assessment of heat and mass transfer of moist vapour, moving along the curved concave surface of the confuser with a density of ρ_{vp}^{mix}, is manifested through a change in the hydrodynamic flow pattern, namely in the form of a decrease in the transverse (radial) pulsation vapour velocity u_r'. If the Prandtl number is less than one, as for example in the case of diethyl ether vapour Pr = 0.77, and the flow velocity over the evaporator is greater than u > 20 m/s and the dynamic boundary layer is thinner than the thermal boundary layer $\delta < \delta_t$, then the effect of mass forces on the transfer process will affect only in the area of the dynamic boundary layer. In this case, we can write the form of the function f [22, 23, 25, 26] to determine the mass forces for the curved concave surface of the HP's confuser part of the vapour channel in the following form:

$$f = \sqrt{1 - \left(\frac{y}{\ell_t}\right)^2 \left(\frac{\delta_t}{\delta_0}\right)^2 Ri} \quad (50)$$

where δ_t is the characteristic thickness of the thermal boundary layer of the curved concave surface for moist vapour, m; δ is the characteristic thickness of the dynamic boundary layer of the curved concave surface for moist vapour, m; δ_0 is the characteristic thickness of the dynamic boundary layer for a flat flow.

The resulting approximation equations, based on the Richardson number, which is a local characteristic of the moist vapour flow along the curved surface of the HP's vapour channel confuser part, and the value of which varies along the thickness of the boundary layer from zero on the wall surface, to the highest value on the outer boundary of the boundary layer thickness δ, allow us to estimate the required shape of the surface and its radius. The main parameter, called integral and characterizing the effect of curvature on heat and mass transfer and friction during flow along the curved surface of the channel, is the ratio of the boundary layer thickness δ to the radius of the channel curvature R_{ch}. To determine this parameter, characterizing the effect of mass forces, heat exchange and friction on the confuser wall, we present expression (52) in dimensionless form, using the relative value of the vapour density and considering thin boundary layers $\delta/R_{ch} << 1$:

$$Ri = \frac{\delta}{R_{ch}}\left(2\Phi\frac{\partial\Phi}{\partial\xi} + \frac{1}{\tilde{\rho}_{vp}^{mix}}\frac{\partial\tilde{\rho}_{vp}^{mix}}{\partial\xi}\Phi^2\right)\Big/\left(\frac{\partial\phi}{\partial\xi}\right)^2 \quad (51)$$

where $\Phi = u_r / u_0$ ($R_{ch} - \delta$) – dimensionless vapour flow velocity circulation.

Since the vapour density is inversely proportional to temperature, the relative density value in the channel can be written as a ratio of experimental temperature values as follows:

$$\tilde{\rho}_{vp}^{mix} = \frac{\rho_{vp}^{mix}}{\rho_{vp0}^{mix}} \cong \frac{T_0}{T} \quad (52)$$

Let's analyze the temperature dependence of the expression for constructing the Richardson number (51), taking into account the relative temperature values given in (52):

$$Ri = \frac{\delta}{R_{ch}}\left(2\Phi\frac{\partial\Phi}{\partial\xi} + \Phi^2\frac{\psi-1}{\psi+\theta(1-\psi)}\frac{\partial\theta}{\partial\xi}\right)\Big/\left(\frac{\partial\Phi}{\partial\xi}\right)^2 \quad (53)$$

where the dimensionless values of the confuser wall surface temperature ψ, or the non-isothermicity factor, and the value of the temperature load θ (or temperature profile) are represented in the following expression:

$$\psi = \frac{T_{wall}}{T_0};\ \theta = (T - T_{wall})/(T_0 - T_{wall}) \quad (54)$$

Since the temperature profiles and the dimensionless circulation of the moist vapour flow velocity in a curved channel are similar, $\Psi \sim \theta$, which is confirmed by the results of numerous experimental studies of flows in curved channels [27-29], they can be equated with each other and represented as a power decomposition by a dimensionless height parameter $\xi = y/\delta$, inside the boundary layer:

$$\Phi = \theta = \xi^n \quad (55)$$

After performing the transformations, taking into account the proposed power decomposition, we write down the expression for calculating the Richardson number in expressions (51) in the following form:

$$Ri = \frac{\delta}{R_{ch}}\left(\frac{2\xi}{n} + \frac{\xi}{n}\frac{\psi-1}{\psi/\theta-(\psi-1)}\right) \quad (56)$$

The exponent n in the velocity circulation profile in (55) is a value, determined on the basis of experimental data and depends on δ / R_{ch}. In the first approximation [26, 30-31] it is usually taken n ~ 1/7 The results of calculations the turbulent heat and mass transfer and friction on a concave surface with a longitudinal radius of curvature R_{ch} of the HP's vapour channel confuser part, under conditions of adiabatic thermal insulation and the absence of the heat losses in a vacuum adiabatic calorimeter, in a limited range of the dimensionless thickness of the boundary layer δ:

$$0 < \frac{\delta}{R_{ch}} \le 0.03 \quad (57)$$

allow you to simplify the expression for calculating the Richardson number (57) as follows:

$$Ri = \frac{2\,\delta\,\xi}{R_{ch}}\frac{(1+n)(1+2n)}{n^2} \quad (58)$$

With a limited velocity value and a small value of the Richardson number for the vapour flow in the confuser part of the vapour channel, the value of the effective radius of curvature R_{ef} of the confuser part of the vapour channel arises and can be evaluated as follows. The ratio of the effective R_{ef} and geometric radii of curvature R_{ch} of the confuser section of the vapour channel allows us to estimate the required geometric radius as follows [28]:

$$d\left(\frac{1}{R_{eff}}\right)/dz \sim \frac{1}{10\delta}\left(\frac{1}{R_{ch}} - \frac{1}{R_{eff}}\right) \quad (59)$$

For a small longitudinal lengths s of the curved concave surface of the confuser section of the HP's vapour channel above the evaporator, equation (59) can be simplified and the geometric radius R_{ch} can be estimated by the formula (60):

$$\frac{1}{R_{eff}} = \frac{1}{R_{ch}}\left[1 - \exp\left(-\frac{s}{10\delta}\right)\right] \quad (60)$$

Estimation of the Reynolds number [16, 17], based on the obtained values of the maximum average velocity of the moist vapour flow between the evaporator surface and the critical section of the HP's vapour nozzle $u_{vp} \sim (30 + 100) / 2 \sim 65$ m/s; the characteristic diameter of the evaporator $D_{ev} = 2 \cdot 10^{-2}$ m, tabular values of the moist vapour density $\rho_{vp}^{mix} \sim 3$ kg / m^3; coefficient of the moist diethyl ether vapour dynamic viscosity $\eta_{mix} \sim 8 \cdot 10^{-6}$ Pa·s, does not exceed the following value of the Reynolds number:

$$Re = \frac{\rho_{vp}^{mix} u_{vp} D_{ev}}{\eta_{mix}} \leq 4.9 \cdot 10^5 \quad (61)$$

With such a Reynolds number and the corresponding thickness of the boundary layer $\delta \sim 1$mm (10^{-3} m), the geometric radius of curvature of the confuser part of the vapour channel does not exceed $R_{ch} \sim (0.8 \div 1) \cdot 10^{-2}$ m. The resulting calculation result and the characteristic geometric radius R_{ch}, which determines the confuser part surface shape of the HP's vapour channel for a closed nozzle with two end flat caps, is close to the real maximum radius of the vapour channel of our short HP's, $R_{ch} = 1 \cdot 10^{-2}$ m.

The expanding (diffuser) fragment of the Laval nozzle, operating in the condensation mode of the vapour flow of short low-temperature HP's, is also limited to the region of subsonic velocities of the moist vapour flow and small values of the Richardson number Ri.

The developed methods [32-35] make it possible to replace the difficult calculation of the curved contour of the diffuser part of the nozzle with a close to parabolic shape of the nozzle surface, while maintaining the parallelism of the vapour flow velocity vectors in the diffuser part of the vapour channel and the longitudinal axis of the nozzle. This makes it possible to significantly simplify all the work on the mandrels manufacture, necessary for the molding the multilayer mesh porous inserts with an internal channel, made like the diffuser section of the Laval nozzle:

$$\Omega(\bar{z}) = (\bar{R}(z) + 1)\sqrt{1 - \left(\bar{R}(z)\right)^{-2}}; \bar{z} = \frac{z}{R^*}; 1 \leq \bar{z} \leq 44 \quad (62)$$

The radius of the vapour channel in the dimensionless form $\bar{R}(z)$ in the diffuser part of the nozzle from the critical section R * = 2 mm to the HP's upper cover, is calculated in the usual way according to the standard formula:

$$\bar{R}(z) = \frac{R_{ch}(z)}{R^*};\ R_{ch}(z) = \sqrt{\frac{1}{2}(x^2 + y^2)} \quad (63)$$

where z is the longitudinal coordinate inside the vapour channel, m.

The profiles of the vapour nozzle-liked channel can be made according to the formula (62) and the equations, given in the book [32]. Thus, the vapour nozzle of our short linear HP's consists of two concave sections, the shape of the surface of which is described by expressions (60) and (62).

3. The Hydraulic Resistance Coefficient of the HP's Vapour Channel

3.1. The Description of the Turbulence Models

Calculations and modeling of the swirling moist vapour flows over a HP's flat evaporator, require careful and adequate selection of a turbulence model. Currently, there are many professional and commercial software systems for modeling various kinds of complex, including turbulent flows. All of them contain basic turbulence models. In this paper, swirling vortex structures are modeled in the ANSYS Fluent package. This is a universal software package for solving problems of fluid and gas mechanics, which provides adequate modeling of complex vortex flows, containing a k-ε turbulence model, which is the most optimal for analyzing condensed vapour flows in HP's. During the calculations, the k-ε turbulence model recommended in the Fluent User's Manual, Version 6.0, was used, the kinetic energy k and the dissipation rate ε of which were calculated using well-known equations recommended by the computational developers [36, 37]:

$$\frac{\partial}{\partial t}(\rho_{vp} k) + \frac{\partial}{\partial x_i}(\rho_{vp} k u_i) = \frac{\partial}{\partial x_j}\left(\left(\mu_{mol} + \frac{\mu_T}{\sigma_k}\right)\frac{\partial k}{\partial x_j}\right) + g_k + g_b - \rho_{vp}^{mix}\varepsilon - Y_M + S_k. \quad (64)$$

$$\frac{\partial}{\partial t}(\rho_{vp} \varepsilon) + \frac{\partial}{\partial x_i}(\rho_{vp} \varepsilon u_i) = \frac{\partial}{\partial x_j}\left(\left(\mu_{mol} + \frac{\mu_T}{\sigma_\varepsilon}\right)\frac{\partial \varepsilon}{\partial x_j}\right) + C_{1\varepsilon}\frac{\varepsilon}{k}(g_k + C_{3\varepsilon} g_b) - C_{2\varepsilon}\rho_{vp}\frac{\varepsilon^2}{k} + S_\varepsilon. \quad (65)$$

In these equations, generally accepted designations are used: g_k - the production of kinetic energy of turbulence due to the gradients of the average velocity; g_b - the production of kinetic energy of turbulence due to the buoyancy of vapour; Y_M - the contribution of fluctuating expansion in the turbulence of compressible vapour to the overall rate of dissipation. C_{1e}, C_{2e}, C_{3e} are constants; σ_k and σ_ε are turbulent Prandtl numbers for k and ε; S_k and S_e are the initial terms, respectively. The effective vapour viscosity coefficient consists of two components: molecular and turbulent. The viscosity of the turbulent vapour μ_t is determined by the standard method in the following form:

$$\mu_{vp} = \mu_{mol} + \mu_t;\ \mu_t = \rho_{vp} C_\mu \frac{k^2}{\varepsilon} \quad (66)$$

where Cμ is a constant, in the standard two equations model k–ε, the turbulence parameters are $C_{1e} = 1.44$, $C_{2e} = 1.92$, $\sigma_k = 1.0$, $\sigma_\varepsilon = 1.3$.

The curvature of the moist vapour current lines near the condensation surface stabilizes the vapour jets and reduces the kinetic energy of turbulence, while a stable toroidal

vortex of condensing vapour is formed, and the direction of rotation of this toroidal vortex depends on the temperature load on the HP's evaporator.

3.2. Calculation of the Hydraulic Resistance Coefficients ξ_{vp} of the Vapour Channel

The effect of partial swirling of the jet vapour stream as a factor affecting the coefficient of hydraulic resistance ξ_{vp} of the flow in the vapour channel of short HP's, made in the form of a Laval nozzle is ambiguous. The flow rotation around the longitudinal axis of symmetry lengthens the trajectories of the vapour micromoles and increases friction losses. The coefficient of hydraulic resistance of the Laval nozzle – liked vapour channel, when a swirling stream of moist vapour flows in it is calculated by the formula (67):

$$\xi_{vp} = \frac{2\Delta P_{vp}}{\rho_{vp}^{mix}(u_z^2+u_r^2+u_\varphi^2)} = \frac{2(P_{ev}-P_{cond})}{\rho_{vp}^{mix}(u_z^2+u_r^2+u_\varphi^2)} \quad (67)$$

For all calculations of the hydraulic resistance coefficient ξ_{vp} of the HP's vapour channel, we take into account the full vapour flow rate in the Laval nozzle –liked channel. The P_{ev} pressure above the evaporator and near the condensation surface P_{cond} is determined and calculated according to [4-6]. In the cylindrical coordinate system r, φ, z, the z axis is directed along the longitudinal axis of the HP's vapour channel, made in the form of a Laval nozzle and, accordingly, along the longitudinal axis of the swirling vortex flow. The analysis of vortex flows and the calculation of the velocity components in the HP's vapour channel will be carried out using a numerical solution in the dimensionless form of the Poisson (68) and Navier-Stokes equations (69) – (71) [9-11, 14, 15] with the generally accepted designations of the current function ψ, vorticity ω= rotu, longitudinal u_z, the radial u_r and azimuthal velocity components u_φ in the following form:

$$\frac{1}{r}\frac{\partial^2\psi}{\partial z^2} + \frac{\partial}{\partial r}\left(\frac{1}{r}\frac{\partial\psi}{\partial r}\right) = -\omega \quad (68)$$

$$\frac{\partial\omega}{\partial t} + \frac{\partial}{\partial z}(u_z\omega) + \frac{\partial}{\partial r}(u_r\omega) = \frac{1}{Re_{vp}}\left[\frac{\partial^2\omega}{\partial z^2} + \frac{\partial^2\omega}{\partial r^2} + \frac{\partial}{\partial r}\left(\frac{\omega}{r}\right)\right] + S^2\frac{1}{r}\frac{\partial u_\varphi^2}{\partial z} \quad (69)$$

$$\frac{\partial u_\varphi}{\partial t} + \frac{\partial}{\partial z}\left(u_z u_\varphi\right) + \frac{1}{r}\frac{\partial}{\partial r}\left(r u_r u_\varphi\right) + \frac{u_r u_\varphi}{r} = \frac{1}{Re_{vp}}\left[\frac{\partial^2 u_\varphi}{\partial z^2} + \frac{1}{r}\frac{\partial}{\partial r}\left(r\frac{\partial u_\varphi}{\partial r}\right) - \frac{u_\varphi}{r^2}\right] \quad (70)$$

$$u_r = -\frac{1}{r}\frac{\partial\psi}{\partial z};\ u_z = \frac{1}{r}\frac{\partial\psi}{\partial r};\ \omega = \frac{\partial u_r}{\partial z} - \frac{\partial u_z}{\partial r} \quad (71)$$

The equations system (68) – (71) of the vapour vortex flow is written in dimensionless form, the longitudinal u_z, azimuthal (tangential) u_φ and radial u_r components of the velocity u are normalized to the longitudinal, azimuthal and radial components of the vapour velocity directly on the surface of the flat evaporator, in the outlet mouths of inclined injection channels according to (1) and [4-6]. The estimation of the vorticity value ω, and the rarefaction ΔP in the center of the vortex with radius r [38, 39] of the condensing vapour gives the following values:

$$\omega \sim \frac{u_v}{r} = \frac{(3-5)\cdot 10^1 m/s}{10^{-2}m} = (3-5)10^3\frac{1}{s};\ \Delta P = (3-5)10^3 Pa \quad (72)$$

On the evaporator surface in the confuser part of the vapour channel, we set the following distributions of the axial u_z, radial u_r and azimuthal u_φ velocity components with restrictions inside the radius r_4, on which the inclined injection vapour channels are made, which set the tangential slope of the vapour jets over the evaporator, and the partial swirling of the vapour flow, similar to those given in [40-43], in dimensionless form:

$$u_z = u_{z0} + u_0\cdot\exp(-b_1 r^2);\ r_4 < r < r_{\Omega(z)}. \quad (73)$$

$$u_\varphi = u_{\varphi 0} + \frac{u_0}{r/r_4}[1-\exp(-b_2 r^2)];\ r_4 < r < r_{\Omega(z)}. \quad (74)$$

$$u_r = u_{r0} + \frac{u_0}{r/r_4}[1-\exp(-b_3 r^2)];\ r_4 < r < r_{\Omega(z)}. \quad (75)$$

where r_4 is the radius, on which the four injector channels in the evaporator are located, m; $r_{\Omega(z)}$ is the radius of the solid wall of the CPI near the evaporator, m; u_{z0} – is the longitudinal component of the vapour velocity directly above the evaporator, m/s; u_{r0} – is the radial component of the vapour velocity directly above the evaporator, m/s; $u_{\varphi 0}$ – is the circumferential the component of the vapor velocity directly above the evaporator, m/s.

Formulas (73) – (75) were proposed earlier by Bachelor [44] from a self—similar solution of the Navier-Stokes equations for a viscous swirling trace of a swirling flow, in a simple plane-parallel geometry of the problem. The sharp profile of the longitudinal and tangential jet components of the vapour velocity inside the diameter $2r_4$ can be considered by quadratic function, which exactly corresponds to the previously proposed and tested calculation options [39] in the following form:

$$u_z = a_0 + a_1\cdot r + a_2\cdot r^2;\ 0 < r < r_4. \quad (76)$$

$$u_\varphi = b_0 + b_1\cdot r + b_2\cdot r^2;\ 0 < r < r_4\ . \quad (77)$$

All polynomials coefficients a_i and b_i are determined from the condition of the vapour sticking to the confuser section surface, and the continuity of the velocity components and their derivatives near the radius of the injection channels r_4 in the evaporator. The input data determining the development of the vapour flow in the entire nozzle area is given as:

$$u_z = u|_{z=0}(r);\ u_r = u_r|_{z=0}(r);\ u_\varphi = u_\varphi|_{z=0}(r). \quad (78)$$

To solve the system (68) – (71), the conditions for ψ, ω and u_φ must be set on the entire solid surface of the vapour channel as follows:

$$\frac{\partial\psi}{\partial z} = \frac{\partial\omega}{\partial z} = \frac{\partial u_\varphi}{\partial z} = 0 \quad (79)$$

The current function ψ can be determined up to a constant value, so we assume that ψ = 0 on the axis of the vapour

channel at r = 0. Therefore, on the axis of the channel at r=0:

$$\psi = 0;\ \omega = 0;\ u_\varphi = 0;\ 0 \le z \le L_{HP} \qquad (80)$$

On the solid side surface Ω=Ω(z) of an axisymmetric vapour channel for a swirling flow, adhesion conditions are realized in the following form:

$$\psi = \psi_{\Omega(z)} = \text{const}; \frac{\partial u_\varphi}{\partial r} = 0; \omega = 0; 0 \le z \le L_{HP}; r = r_{\Omega(z)} \qquad (81)$$

The algorithm of the numerical solution of the equations system (68) – (71) and calculation the current function, vortices and vapour flow velocities is standard [39-41], and consists in the sequential determination, starting from zero, of all these quantities in steps along the coordinate h and in time Δτ, using the equations in finite differences with homogeneous boundary conditions.

Calculations of the desired parameter value are stopped when the relative difference between the subsequent and previous values of the calculated value differ from each other by less than $5 \cdot 10^{-3}$. The numerical result is considered achieved. All details of the solution of the Poisson (68) and Navier–Stokes (69) – (71) equations are given in [39, 41].

The momentum flow of the amount of vapour movement in the axial direction $M_{z\varphi}$ and the momentum flow (amount of motion) M_z of vapour in the axial direction are determined in the usual way:

$$M_{z\varphi} = \int \rho_{vp}^{mix} u_z u_\varphi \, r d\Omega;\ M_z = \int \rho_{vp}^{mix} u_z^2 \, d\Omega \ . \qquad (82)$$

The integration boundary surface is the surface of the solid wall of the nozzle Ω(z), starting from the value of the radius of the evaporator R_{ev}, then up to the critical diameter of the nozzle d_{cr} and the radius of the HP's condensation surface R_{cond}.

The parameter S of the vapour flow swirling above the evaporator is determined by the values of the moment flows of the amount of vapour movement and the value of the vapour momentum flow, or the component of the vapour flow velocity directly above the four inclined injector channels of the evaporator, setting the angle of inclination φ of the w_{vp} component above the evaporator as follows:

$$S = \frac{M_{z\varphi}}{M_z \cdot r_4} \cong \frac{w_{ev}}{u_{ev}} \ . \qquad (83)$$

Taking into account the radius of the injection channels r_4, the radius of the evaporator R_{ev}, m; the thickness of the evaporator L_{ev}, m; and the length of the confuser section of the channel L_{conf}, m; the integral parameter of the swirling can be written as follows:

$$S = \left(\frac{1}{1+r_4/R_{ev}} + \frac{L_{ev}}{L_{conf}}\frac{r_4}{R_{ev}}\right) tg\varphi. \qquad (84)$$

With the swirling flow of vapour jets, the current lines of the averaged flow are helical lines, the radius of curvature of which R_{ch}, depends on the swirling angle of vapour jets φ [48], and the radial coordinate r as follows:

$$R_{ch} = \frac{r}{\sin^2\varphi(r)} = r\left(1 + \frac{1}{tg^2\varphi}\right) = r\left(1 + \frac{u_z^2(r)}{u_\varphi^2(r)}\right); \varphi = \text{arctg}\left(\frac{u_\varphi(r)}{u_z(r)}\right) \qquad (85)$$

The maximum value of the integral parameter S of the vapour jet flow swirling over our flat evaporator can reach the value S = 1.52.

The hydraulic resistance coefficient ξ_{vp} of the HP's vapour channel with a flat covers, was calculated according to the procedure, recommended in Russian technical standards GOST RF R 55508-2013 [42] and RD RF 26-07-32-99 [43], according to the formula (67). Figure 8 shows the obtained calculated results of the hydraulic resistance coefficient ξ_{vp}, made in the form of a Laval-liked nozzle with concave walls, and a vapour channel, closed with flat covers, with injection jet streams of diethyl ether vapour in the velocity range of 1 – 100 m/s, and in the range of Reynolds numbers $Re_{vp} = 10^3 – 10^5$.

By calculation, we have recorded the existence of a range of values of the partial swirling coefficient of the flow S ≤ 0.5, for a moist stream of vapour above the evaporator in the HP's vapour channel, at which the coefficient of hydraulic resistance (hydraulic friction) decreases compared with a hydraulic resistance of the purely translational jet vapour flow with equivalent Reynolds number, [41-43]. The minimum values of the hydraulic resistance coefficient ξ_{vp} made in the form of a Laval-liked nozzle in the vapour channel of short HP's with flat covers, starting with a vapour flow velocity of 10 m/s, are set by us at a swirling angle φ = (26-28) °. Figure 8 shows the obtained results.

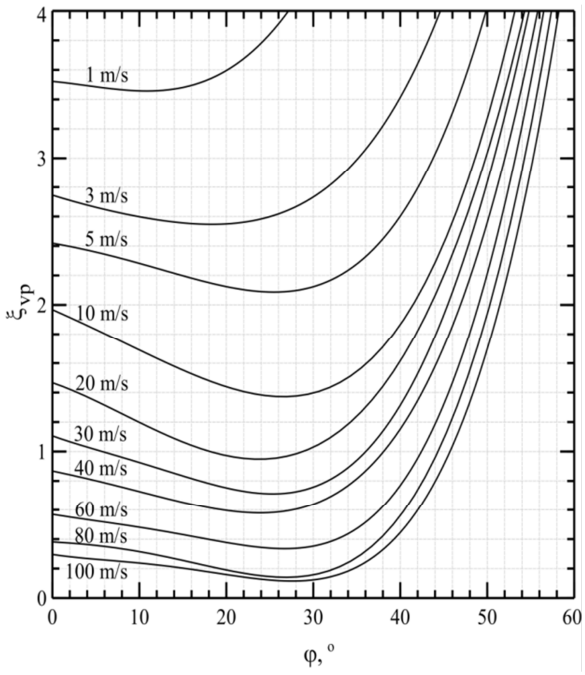

Figure 8. *Dependence of the hydraulic resistance coefficient ξ_{vp} of the vapour channel, closed by the flat lids with injected jet flows at different slope angles φ in the range of Reynolds numbers $R_{evp} = 10^3 - 10^5$. The figures on the curves in the left part of the figure mean the average velocity of vapour flow in the HP's vapour channel, m/s.*

A reduction value is up to 40%.

4. Experimental Determination of the Heat Transfer Coefficients K_{HP}

Nine additional HP's were created with identical dimensions and diethyl ether filling mass, δm/m ≤. 0.1%. The manufacturing errors of flat evaporators, injector channels with angles of inclination φ did not exceed the standard ones, the error of setting the angles of inclination of channels δφ ≤ not more than 0.5°.

To analyze the characteristics and peculiarities of vortex swirling vapour flow in the HP's channel, and to compare the experimental values of heat transfer coefficients of K_{HP}, a vortex flow calorimeter was used, the design of which was described earlier [4-6], all measurements were carried out under normal conditions, atmospheric pressure and ambient temperature $T_0 = 293$ K.

The heat transfer coefficient K_{HP} of our HP's, according to Faghri [45], is determined by formula (86):

$$K_{HP} = \frac{q_{ev} - h_{fr} - k^0_{TT}(\overline{T}_{HP} - T_0)}{F_{ev}(z)(T_{ev} - T_{cond})}. \quad (86)$$

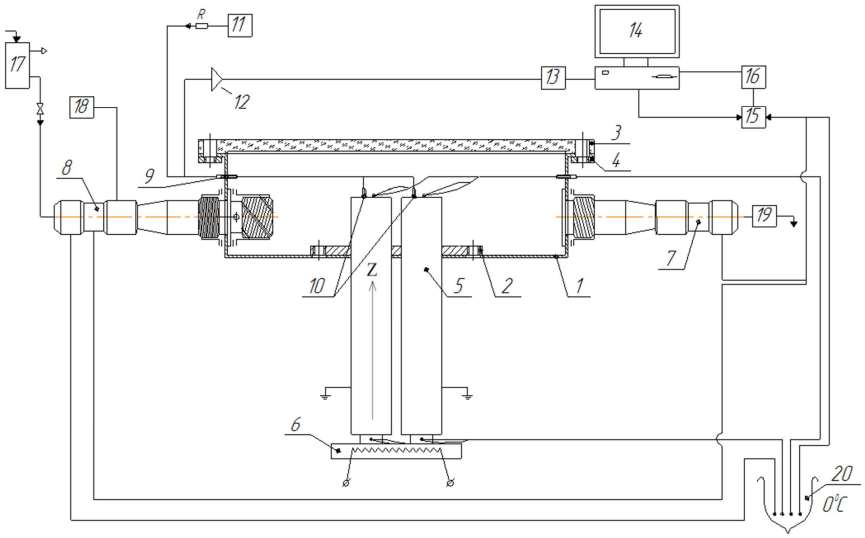

Figure 9. *Schematic diagram of the vortex flow calorimeter designed for measurements the heat transfer coefficient K_{HP} of short linear HP's under normal conditions, without adiabatic and vacuum insulation. 1-vortex flow calorimeter; 2- HP's mounting flange; 3- glass cover; 4- cover fastening; 5- support HP's filled with dried air at atmospheric pressure and the second HP's, completely identical to the first one, and called measuring HP, filled with diethyl ether; 6-flat resistive heater; 7-drain connection of the calorimeter; 8-inlet connection - calorimeter swirler; 9-sealed inlet of measuring wires; 10-capacitive sensor for measuring the modulation frequency in the left HP, in the right HP a similar sensor; 11-external quartz pulse generator; 12- amplification and filtering circuit; 13-digital oscilloscope; 14-computer PC; 15-a digital voltmeter; 16-a controlled switch based on reed relays RES-44; 17-a constant water head vessel; 18-a generator of air bubbles; 19-a flow meter US 800-10; 20- Dewar vessel, realizing the 'zero point' of 0°C.*

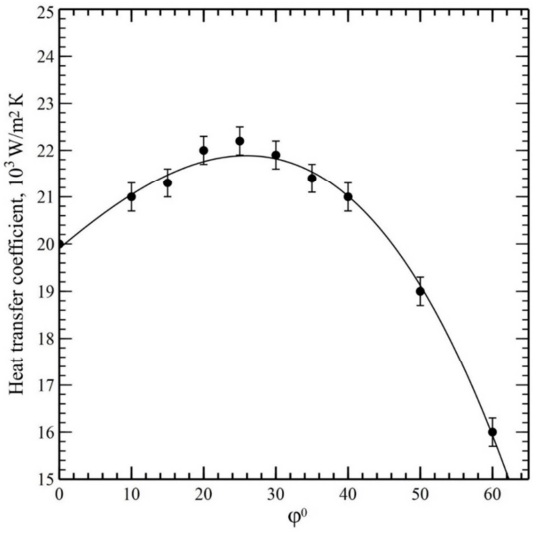

Figure 10. *Heat transfer coefficient of short HP's as a function of the geometric angle of inclination φ° of the injection channels in the evaporators, and at the same temperature load on the evaporator $\delta T = T_{ev} - T_B = (20 \pm 0.03)$ K.*

Energy losses by vapour friction h_{fr} in the vapour channel of short linear HP's were estimated earlier [4-6] using an adiabatic vacuum calorimeter, combined with a vortex flow calorimeter, in which the HP's energy losses for heat exchange do not exceed $(0...1)\cdot 10^{-2}$ W.

Heat losses of the outside cylindrical surface of the HP's, made of stainless steel 1X18H9T, with the average surface temperature $\overline{T}_{TT} = (293 \dots 373)$K, due to heat exchange with the environment at room temperature 293 K and atmospheric pressure, are estimated in the usual way [6]:

$$k^0_{TT}(\overline{T}_{HP} - T_0) = (0 \dots 0.125)\frac{W}{K}\cdot(\overline{T}_{HP} - 293)K = (0 \dots 10)W, \quad (87)$$

All details of the measurements with regard to heat transfer, including the characteristics of the vortex flow calorimeter, are given in [4-6].

Figure 10 shows the obtained results of comparing the heat transfer coefficients K_{HP} of the identical HP's with differing only in the angles of inclination of the evaporator injection channels at the same temperature load on the evaporator $\delta T = T_{ev} - T_B = (20 \pm 0.03)$ K.

All details of the measurements with regard to the heat transfer, including all characteristics of the vortex flow calorimeter, are given in [4-6].

5. Results and Discussion

As a result of the analysis of obtained data, presented in Figure 10, where each point represents the experimentally determined value of the K_{HP} of a separate short HP, with made in the form of the Laval nozzle-liked concave vapour channel, with identical overall dimensions and mass of filling with diethyl ether ($\Delta m/m < 0.1\%$), with a given angle of inclination of the injector channels and at the same temperature load $\delta T = T_{ev} - T_B = 20K$, it was concluded, that the maximum of the functional dependence of the heat transfer coefficient, takes place at the vapour flow swirling angle $\varphi = 26° \pm 2°$. The increase of the HP's heat transfer coefficients K_{HP} at a partial swirling vapour flow above the HP's evaporator, using the inclination of the injector channels with a diameter of 1 mm is due to several reasons.

First, the main reason is the occurrence of an additional azimuthal rotation of the toroidal vortex of condensing vapour, formed near the flat condensation surface - the surface of the HP's top cover, clearly fixed in Figure 11. Azimuthal rotation of the toroidal vortex, leads to an additional decrease of static pressure at its center on the longitudinal axis, and an increase of pressure drop in the HP's vapour channel between the evaporator and the center of the toroidal vortex.

Secondly, the reduction of the hydraulic resistance coefficient ξ_{vp} of the profiled vapour channel at movement in it the swirling jet flow of moist vapour, limited by the flat covers of the short HP's is obtained by calculations, and the minimum value of the ξ_{vp} is fixed near the swirling angle $\varphi = 26° \pm 2°$, see Figure 8.

To evaluate the effect of additional azimuthal rotation of the toroidal vortex of condensing vapour, in addition to its resulting axial rotation [5, 6], it is necessary to estimate the calculated values of the azimuthal velocity and pressure change in the center of the toroidal vortex.

Figure 11 shows the rotational flow of a vapour in the HP's vapour channel.

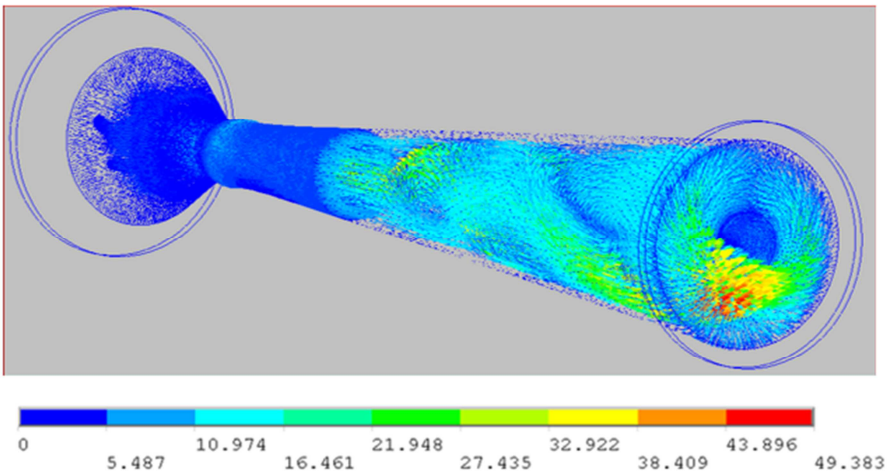

Figure 11. *Partially swirled vapour flow in the vapour channel and near the HP's condensation surface, confirming the non-zero value of the azimuthal rotation velocity of the toroidal vortex of condensing vapour.*

A qualitative analysis of the toroidal vortex flow in the HP's vapour channel can be performed using the Helmholtz equation, describing the change in the vorticity of the formed toroidal vortex structure near the vapour condensation surface, in the following form [14, 15]:

$$\frac{\partial \omega}{\partial t} + (u \cdot \nabla)\omega = (\omega \cdot \nabla)u + \nu_{vp}^{mix} \nabla^2 \omega. \qquad (88)$$

This equation relates the change in the vorticity ω of a mole of moist vapour, moving along the current line (left-hand side) to the stretching or contraction of the toroidal vapour vortex under confined channel conditions, and to the diffusion of the vorticity. The first term on the right side can be divided into a component along the current line causing stretching or compression of the vortex, and a component perpendicular to the current line causing a change in the orientation of the swirl vector ω.

Vortex compression is possible, when the longitudinal acceleration of the vapour flow in the channel is changed, when the temperature load on the HP's evaporator is increased, and when it is additionally rotated azimuthally as a whole.

To evaluate the effect of azimuthal rotation of the vapour vortex near the condensation zone inside the HP, the value of the azimuthal rotation velocity of a toroidal vapour ring, with average radius R_0, inside the vapour channel, was calculated using the Mac - Cormack formula [46, 47].

Figure 12. shows the distribution of the circumferential velocity of an axisymmetric vapour vortex in addition to the axial velocity $u \sim u_{vp}$. We use the maximum value of the circumferential velocity of the toroidal vortex of 10 m/s, the energy density of the circumferential rotation in the vortex is approximately equal:

$$E = \frac{1}{2}\rho_{vp}^{mix} u_{cir}^2 \sim \frac{1}{2} 3.3 \cdot 10^2 = 1.65 \cdot 10^2 \frac{J}{m^2} \qquad (89)$$

Figure 12 shows the calculated value of the azimuthal velocity of the toroidal vortex condensing diethyl ether vapour [15, 46, 47], the maximum of the azimuthal velocity is at $r/R_0 = 1$.

Figure 13 shows the calculated values of the pressure change ΔP at the center of the toroidal vortex condensing diethyl ether vapour in the HP's vapour channel.

The dependence of the relative pressure decrease in the center of the toroidal vortex on the vortex radius using the McCormick formula is calculated as follows:

$$\Delta P_{cir}(r) = \frac{\left[P(T_{cond}) - \frac{1}{8\pi^2}\frac{\rho_{vp}^{mix}\Gamma^2}{(r^2+R_0^2)F(z)}\right]}{P(T_{cond})} \quad (90)$$

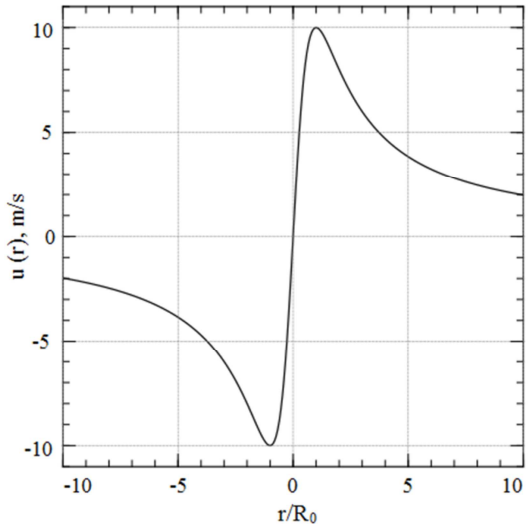

Figure 12. *Calculated values of the azimuthal velocity of the annular vortex u(r), m/s; R_0 is the radius of the vortex, m; r is the distance from the centerline of the HP's vapour channel, m.*

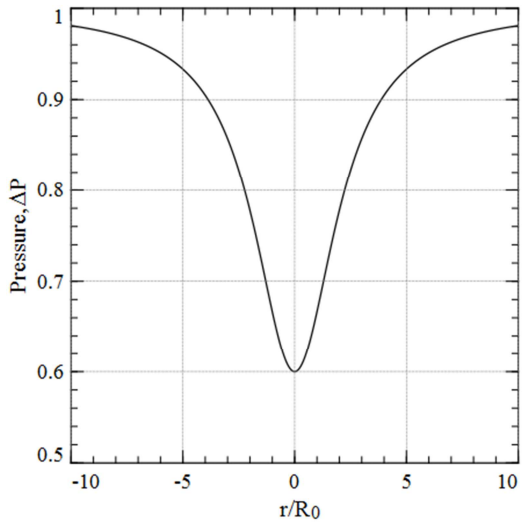

Figure 13. *Additional relative pressure change in the center of the toroidal vortex of condensing vapour due to azimuthal rotation of the vortex near the flat surface of the top cover of the HP, leading to an increase in the heat transfer coefficient of short HP's with inclined injection channels in a flat evaporator. This decrease of static pressure in the center of the axial toroidal vortex ring, with its additional azimuthal rotation, leads to an increase in the heat transfer coefficient of short HP's with inclined injection channels in a flat evaporator.*

$\Gamma = 2\pi R_0 u_{cir}$ is the azimuthal circulation of the vortex, m^2/s; $P(T_{cond})$ is the vapour pressure inside the vortex near the condensation surface without azimuthal rotation, Pa.; F(z) is the area of the condensation surface, m^2.

When the azimuthal circulation value of the vapour vortex inside the HP channel is of the order of $\Gamma \sim 0.01$ m^2/s, the additional relative pressure drop inside the vortex reaches 0.4 $P(T_{cond})$.

6. Conclusions

1. The use of a swirling flow in the Laval nozzle–liked vapour channel, in a limited range of the swirling angles $\Delta\varphi < 30$ ° of vapour jets above the evaporator, reduces the coefficient of hydraulic resistance for the jets flow in the vapour channel up to 40% compared to the HP's with a direct-flow vapour jets.
2. An experimental comparison of the heat transfer coefficients KHP of short identical HP's with a Laval nozzle–liked vapour channel, the same mass of diethyl ether filling, differing only in the different angle of inclination of the injection channels of a multilayer flat evaporator, showed an increase in KHP up to 10% at a swirling angle (26 ± 2) °.
3. The reason for the increase in KHP is the additional azimuthal swirling of the resulting toroidal vortex of condensing vapour near the flat surface of the HP's upper cover – the condensation surface. Azimuthal rotation of a toroidal vortex with a standard axial swirling, leads to a decrease in vapour pressure in the central part of the vortex ring, and thereby to an increase in the pressure drop in the HP's channel between the evaporator and the center of the condensing vapor vortex. The value of additional pressure reduction in the center of the toroidal vortex of condensing vapour may reaches 0.4 P (Tcond).

Nomenclature

C_p^{mix}: heat capacity of moist vapour, J/kgK;

D: diameter of the HP's vapour channel, m;

$F(\bar{z})$: cross-sectional area of the HP's, m^2;

h_{fr}: friction energy losses in the vapour channel and in the liquid subsystem of the HP's, W;

k_{TT}^0: heat exchange coefficient of the HP's surface with the environment, W/K:

ℓ_0: mixing path length at vapour flow on a flat surface without swirling, m;

ℓ: length of the turbulent mixing path for the curvilinear boundary layer, m;

L_{HP}: length of the HP, m;

L_{ev}: thickness of CPE, m

P_{ev}: vapour pressure above the evaporator, Pa;

P_{cond}: vapour pressure above the condensation surface, Pa:

q_{ev}: heat power entering to the CPE, W;

q_{cond}: heat power released at the condensation surface, W;

r: variable coordinate along the vapour channel radius, m;

$r(T_B)$: specific heat of vaporization of diethyl ether, kJ/kg;

R(z): radius of the vapour channel of HP's, m;

R_{ch}: curvature radius of the confuser part of vapour channel, m;

$R_{HP}(t)$: thermal resistance of the HP's, K/W;

Re_{eff}: effective Reynolds number of swirling moist vapour flow in the HP's vapour channel;

$Re = u_{zo}\rho_{vp}^{mix}D/\mu_{vp}^{mix}$: Reynolds number of longitudinal moist vapour flow in the HP's vapour channel;

Re**: Reynolds number determined by the thickness of momentum loss δ** of the moist vapour flow moving along the HP's concave confuser surface;

Ri: Richardson number of moist vapour flow;

$tg\varphi = u_\varphi / u_{z0}$: angle of the vapour flow swirling, determined by the ratio of azimuthal and longitudinal velocity components, °;

T_0: the average outlet temperature of vapour at the outer boundary of the boundary layer, which in the first approximation can be considered equal to the vapour temperature above the HP's evaporator, K;

T: temperature of the moist vapour flow, K;

T_B: boiling point of diethyl ether;

T_{cond}: temperature of the condensation surface of TT, K;

T_{ev}: temperature of the grid evaporator saturated with working liquid, K;

T_{sc}: temperature of the grid frame of the CPE, K;

T_{wall}: temperature of the vapour channel wall, K;

T': pulsation component of the moving vapor temperature, K;

u: flow velocity of the moist vapour flow in the condensation zone in the HP's vapour channel, m/s;

u_{zo}: flow-averaged longitudinal component of the moist vapour velocity in the HP's channel, m/s;

u_z: longitudinal component of the vapour flow velocity in the HP's vapour channel, m/s;

u_r: radial component of the vapour flow velocity in the confuser part of the HP's vapour channel, m/s;

u'_r: radial component of vapour pulsation velocity, m/s;

z, y: coordinates, directed respectively, along the surface downstream and normal to it (inside the boundary layer thickness δ), m.

x_{ev}: degree of vapour dryness in the CPE;

β: dimensionless constant value;

δ: thickness of the boundary layer of the moist vapour flow inside the HP's vapour channel, m;

δ**: dynamic thickness of momentum loss of moist vapour flow inside the HP's channel, m;

δ**/R: dimensionless longitudinal curvature of the channel surface;

$\theta = (T-T_{wall}) / (T_0: T_{wall})$: dimensionless temperature profile on the wall;

λ_{sc}: heat conductivity coefficient of the CPI mesh frame, W/mK;

λ(t): HP's thermal conductivity coefficient, W/m-K;

μ_{vp}^{mix}: dynamic viscosity coefficient of moist vapour in the HP's vapour channel, Ps·s;

$\xi = y / \delta$: dimensionless normal coordinate y in the boundary layer thickness;

ρ_{vp0}^{mix}: average discharge density of moist vapour above the evaporator, kg / m^3;

ρ_{vp}^{mix}: density of the moist vapour inside the HP's vapour channel, kg/m^3;

$\tilde{\rho}_{vp}^{mix}$: relative density of the moist vapour inside the vapour channel;

ρ_{vpev}^{mix}: density of the moist vapour directly above the evaporator, kg / m^3.

$\tilde{\tau}_0 = (\tau/\tau_{wall})_0$: profile of tangential stresses during the flow of moist vapour under standard conditions (flat impermeable wall under isothermal conditions);

$\tilde{\tau} = (\tau/\tau_{wall})$: profile of tangential stresses at moist vapour flow on the HP's wall;

Ψ - relative friction function of moist vapour flow on the HP's vapour channel;

ψ_k - relative coefficient of friction of moist vapour flow, taking into account the influence of longitudinal curvature of the vapour channel surface;

ψ_t - relative friction coefficient of moist vapour flow, taking into account the influence of non-isothermicity of the vapour channel surface;

$\bar{\omega}_0$: dimensionless velocity circulation in a flat isothermal vapour channel.

Π: porosity coefficient of CPE and CPI.

Acknowledgments

The author expresses his gratitude to Academician A. A. Khalatov for initiating this work to study the influence of swirling flows in the Laval nozzle-shaped vapour channel of short HP's, on the value of heat transfer coefficient K_{HP}.

References

[1] Gerasimov Yu. F., Maidanik Yu. F., Shchegolev G. T., Filippov G. A., Starikov L. G., Kiseev V. M., Dolgirev Yu. E. Low-temperature heat pipes with separate channels for vapour and liquid. // Engineering Physics Journal, 1975, v. 28, N. 6, pp. 957-960.

[2] Tong B. Y., Wong T. N., Ooi K. T. Closed-loop pulsating heat pipe// Applied Thermal Engineering, 2001, v. 21, № 18, pp. 1845-1862.

[3] Akachi H. Structure of Heat Pipe. US patent 4921041. 1990.

[4] Seryakov A. V. Intensification of heat transfer processes in the low temperature short heat pipes with Laval nozzle formed vapour channel //American Journal of Modern Physics 2018, v. 7, № 1, pp. 48-61.

[5] Seryakov A. V. Computer modeling of the vapour vortex orientation changes in the short low temperature heat pipes //International Journal of Heat and Mass Transfer 2019 v. 140. pp. 243-259.

[6] Seryakov A. V. Resonant vibration heat transfer coefficient increase of short low-temperature heat pipes //International Journal of Heat and Mass Transfer 2020. v. 158. pp. 1-22. Article *119764.*

[7] Goldstick M. A. Vortex flow. - Novosibirsk: Nauka, 1981. - 336 p.

[8] Alekseenko S. V., Kuibin P. A., Okulov V. L. Introduction to the theory of concentrated vortices. Novosibirsk: Institute of Thermophysics 2003, 504 p.

[9] Khalatov A. A. Theory and practice of swirling flows. Kiev: Naukova Dumka 1989. 192 p.

[10] Gupta A., Lilly D., Sayred N. Swirled Flows. Moscow: Mir, 1987. 588 p.

[11] Shchukin V. K. Heat exchange and hydrodynamics of internal flows in the fields of mass forces. -M.: Mashinostroenie, 1980. – 240 p.

[12] Shchukin V. K., Khalatov A. A. Heat transfer, mass transfer and hydrodynamics of twisted flows in axisymmetric channels. - M.: Mashinostroenie, 1982. -200 p.

[13] Kholodkova O. Yu., Fafurin A. V. Experimental study of heat transfer in a cylindrical channel in the presence of initial swirling and blowing of various gases. - In the book Heat and Mass Exchange in Aircraft Engines. Proceedings of KAI. Kazan, 1974, v. 178, pp. 20-27.

[14] Loytsyansky L. G. Mechanics of liquid and gas. 7th ed. - M: 2003. – 840 p.

[15] Landau L. D., Lifshits E. M. Theoretical Physics in 10 volumes. Volume 6. Hydrodynamics. -M: Nauka, 1986. – 736 p.

[16] Seryakov A. V. The solving of the inverse thermal conductivity problem for study the short linear heat pipes // Engineering 2022, v. 14, pp. 1-32.

[17] Seryakov A. V., Alekseev A. P. Solution of the Inverse Problem of Heat Conduction for Investigation of Short Linear Heat Tubes// Vestnik of the International Academy of Refrigeration 2022 №1. pp. 83-97.

[18] Kutateladze S. S., Leontiev A. I. Heat and Mass Exchange and Friction in Turbulent Boundary Layer. M.: Energia. 1972. 376c.

[19] Prandtl L. Gesamelte Abhandlungen. Berlin u. a. Springer-Verlag, 1961, Bd. 2, pp. 798-811.

[20] Bradshaw P. The analogy between streamline curvature and buoyancy in turbulent shear flow. Journal of Fluid Mechanics 1969. v. 36, pt. 1, pp. 177-191.

[21] Kutateladze S. S., Volchkov E. P., Terekhov V. I. Aerodynamics and Heat and Mass Transfer in Limited Vortex Flows. Novosibirsk: IT SB AN USSR. 1987, 282 p.

[22] Gostintsev Yu. A. Heat and mass transfer and hydraulic resistance in the course of a rotating liquid flow through a pipe// Izvestiya AN USSR Mekhanika Zhidkosti i Gaza. 1968, № 5, pp. 115-119.

[23] Migai V. K., Golubev L. K. Friction and Heat Exchange in a Turbulent Swirled Flow with Variable Torsion in a Pipe// Izvestiya AN USSR Energetika i Transport. 1969, No. 4, pp. 141-145.

[24] Seryakov A. V., Alekseev A. P. A Study of the Short Heat Pipes by the Monotonic Heating Method. 2020// Journal of Physics: Conference Series 1683 022051.

[25] Corino E. R., Brodkey R. S. A visual investigation of the wall region in turbulent flow// Journal of Fluid Mechanics 1969, v. 37, № 1, pp. 1-30.

[26] Shchukin, A. V. Turbulent boundary layer on a curvilinear surface (in Russian) // Izvestiya Vuzov. Aviation Engineering. 1978, № 3, pp. 113-120.

[27] Ustimenko, B. P. Turbulent transfer processes in rotating flows. Alma-Ata: Nauka. 1977. 228 p.

[28] Gillis J. C., Johnston J. P., Kays W. M., Moffat R. J. Turbulent boundary layer on a convex, curved surface: Report NHMT-31. Stanford University 1980. 295p.

[29] Bradshaw P. Review. Complex turbulent flows. Transactions ASME. Ser. I, 1975, v. 97, № 2, pp. 146-154.

[30] Wattendorf F. H. A study of effect of curvature on fully developed flow. Proceedings of the Royal Society, London. Ser. A. 1935, v. 148, pp. 565-597.

[31] Mayle R. E., Blair M. E., Kopper F. C. Turbulent boundary layer heat transfer on curved surfaces. Transactions ASME, Journal of Heat transfer 1979. v. 101, № 3, pp. 521-525.

[32] Vasiliev, A. P.; Kudryavtsev, V. M.; Kuznetsov, V. A. et al. Fundamentals of Theory and Calculation of Liquid Rocket Engines. In 2 books. -M: Vyshaya shkola 3rd ed., 1993. Book 1 - 383 p. Book 2 - 368 p.

[33] Brassard D., Ferchichi M. Transformation of polynomial for a contraction wall profile // Journal of Fluids Engineering v. 127. pp. // pp. 183-185. 2005.

[34] Kurokava J., Kajigaya A., Matusi J., Imamura H. Supression of swirl in a conical diffuser by use of J-groove, in: Proc. 20th IAHR Symposium on hydraulic machinery and systems. Charlotte, North Carolina, USA, DY-01. 2000.

[35] Doolan C. J. Numerical evaluation of contemporary low-speed wind tunnel contraction designs // Journal of Fluids Engineering v. 129. pp. 1241-1244. 2007.

[36] CFdesign 10.0 2009. Version 10.0 – 20090623. User's Guide.

[37] Fluent User's Manual, Version 6.0. November 2001.

[38] Kochin N. E., Kibel I. A., Roze N. V. Theoretical Hydromechanics. Part 1. 6th ed. - M: 1963. -584 p.

[39] Akhmetov V. K., Shkadov V. Ya. Numerical modeling of viscous vortex flows for technical applications. MSCU. Moscow 2009. 176 p.

[40] Akhmetov, V. K.; Shkadov, V. Ya. To a question about stability of a free vortex (in Russian) // Vestnik of Moscow State University. Series 1. Mathematics and Mechanics 1987. №2 pp. 35-40.

[41] Akhmetov V. K., Shkadov V. Ya. Development and stability of swirling currents // Izvestia AS USSR. Fluid and Gas Mechanics 1988. №4, pp. 3-11.

[42] GOST RF 34437-2018 Pipeline valves. Methods of experimental determination of hydraulic and cavitation characteristics.

[43] RD RF 26-07-32-99. Pipeline valves.

[44] B a t c h e l o r G. K. Axial flow in a trailing vortices//Journal of Fluid Mechanics 1964. 20, N 4. pp. 645-658.

[45] Faghri A. Heat Pipe Science and Technology. Washington USA, Taylor and Francis. 1995. p. 874.

[46] Bernard Robert. – A McCormack scheme for incompressible flow. – Computers & Mathematics with Applications. 1992. v. 24. No. 5/6. – pp. 151-168.

[47] Hoffman J. D. Numerical methods for engineers and scientists. Second edition revised and expanded. – New York. Marcel Dekker, Inc. – 2001. – 825 p.

[48] Bronstein I. N., Semendyaev K. A. Handbook of Mathematics. - M.: Nauka, 1980. - 976 p.